

Recent developments on the Component Method

Kim J. R. Rasmussen^{*,a}, Xianzhong Zhao^b, Shen Yan^{a,b}, Liusi Dai^{a,b}, Chen Zhu^a, Luli Jiang^a

^aThe University of Sydney, Australia

kim.rasmussen@sydney.edu.au, shen.yan@sydney.edu.au,
liusi.dai@sydney.edu.au, czhu7452@uni.sydney.edu.au, luli.jiang@sydney.edu.au

^bTongji University, China

x.zhao@tongji.edu.cn

ABSTRACT

The Component Method is well established and incorporated in Part 1.8 of Eurocode3 for the design of connections of steel frameworks. It is primarily intended to provide the elastic joint stiffness, although Part 1.8 includes provisions for also determining the inelastic moment-rotation response from the elastic limit to the ultimate moment. The latter provisions are empirical and use an established experimentally-based nonlinear equation to define the inelastic response.

The Component Method has been further developed in recent years to determine the inelastic response using bi-linear springs with elastic and inelastic ranges. Procedures have also been developed at the University of Sydney to extend the Method into the post-ultimate range by defining tri-linear springs with elastic, inelastic and softening ranges. As well, recent research at the University of Sydney has produced a simple way to predict the moment-rotation response under fracture of components, thus enabling the Method to capture the full moment-rotation behaviour. The ability of the Method to predict full-range moment-rotation behaviour is especially useful for design by advanced analysis and progressive collapse analysis, as it allows both members and connections to be checked for stiffness and strength as part of the analysis.

In parallel, an ongoing joint project between Sydney University and Tongji University on the strength of beam-to-upright connections in rack structures has extended to Component Method to cold-formed steel connections which include tang-connectors and bolts. The paper provides an overview of these recent developments of the Component Method, including the opportunity to incorporate the Method in a fully nonlinear procedure for the direct design of steel frameworks including connections by advanced analysis, also referred to as the Direct Design Method.

Keywords: steel connection, component method, full-range response, steel storage rack connection

1 INTRODUCTION

In the past two decades, comprehensive studies have been conducted for the development of the Component Method, which has been incorporated in Part 1.8 of Eurocode3 to determine the elastic stiffness and the ultimate moment of steel joints [1]. However, there are still two significant disadvantages of the current version of the Component Method. First, it does not contain provisions for creating spring-based mechanical models for predicting the inelastic moment-rotation response from the elastic limit to the ultimate moment, nor the response beyond the ultimate moment, including the post-ultimate softening range, and the fracture and the post-fracture ranges; Part 1.8 of Eurocode3 only provides an experimentally-based empirical approach to define the inelastic response up to the ultimate moment. Second, Part 1.8 of Eurocode3 is not readily applied to certain types of cold-formed steel joints, including the beam-to-upright joints in rack structures, because these joints feature components such as tang-connectors which are not covered by Part 1.8 of Eurocode3.

This paper presents recent research at the University of Sydney aiming to extend the Component Method to the inelastic range, and the post-ultimate and the post-fracture ranges, as well as recent joint research between the University of Sydney and Tongji University for extending the Component Method to cold-formed steel connections.

2 GENERALISED COMPONENT METHOD

The context of establishing the Generalised Component Method [2] is to overcome the limitations of the current Component Method incorporated in Eurocode 3 [1] and other available mechanical spring models in the literature [3-4], as mentioned in the Introduction. In particular, the Generalised Component Method specifies the inelastic and softening (negative) stiffnesses of components, as well as their ultimate capacity and ductility. By considering the connection as an assembly of non-linear springs, this allows the inelastic response, ultimate capacity, post-ultimate response and ductility of the complete connection to be determined. The Generalised Component Method also specifies a procedure for determining whether a tension (or compression) component is currently under increasing loading or under unloading, which is important to know because for a nonlinear component the loading and (elastic) unloading responses are different.

2.1 Force-displacement relationship of a spring series

In the Generalised Component Method, as shown in Fig. 1, each spring representing a component of joint can be disassembled into three springs, i.e., an elastic spring, a plastic spring and a softening spring, which are used to reproduce the initial elastic behaviour, the inelastic behaviour and the post-ultimate softening behaviour, respectively. Based on the minimum total potential energy principle, the force-displacement relationship of a series of tri-linear springs can be written as [2]:

$$F = \langle K^j \rangle (\Delta + \langle C^j \rangle) \quad (1)$$

$$\langle K^j \rangle \equiv \begin{cases} K_e^j = \left(\sum_{i=1}^n \frac{1}{k_{e,i}} \right)^{-1}, & F < P_{p,1}^C \\ K_p^j = \left(\sum_{i=1}^n \frac{1}{k_{e,i}} + \sum_{i=1}^m \frac{1}{k_{p,i}} \right)^{-1}, & P_{p,1}^C \leq F < P_{s,1}^C \\ K_s^j = \left(\sum_{i=1}^n \frac{1}{k_{e,i}} + \frac{1}{k_{s,1}} \right)^{-1}, & F = P_{s,1}^C \text{ and subsequent } F < P_{s,1}^C \end{cases} \quad (2)$$

$$\langle C^j \rangle \equiv \begin{cases} C_e^j = 0, & F < P_{p,1}^C \\ C_p^j = \sum_{i=1}^m \frac{P_{p,i}^C}{k_{p,i}}, & P_{p,1}^C \leq F < P_{s,1}^C \\ C_s^j = \sum_{i=1}^m \frac{P_{s,1}^C - P_{p,i}^C}{k_{p,i}} + \frac{P_{s,1}^C}{k_{s,1}}, & F = P_{s,1}^C \text{ and subsequent } F < P_{s,1}^C \end{cases} \quad (3)$$

where n is the total number of springs in the spring series; $k_{e,i}$, $k_{p,i}$ and $k_{s,i}$ are the stiffnesses of the i th elastic spring, the i th plastic spring and the i th softening spring, respectively; $P_{p,i}^C$ and $P_{s,i}^C$ are the critical loads of activation of i th plastic spring and the i th softening spring, respectively; and the superscript j represents different stiffness stages, the total number of which is denoted as N^j .

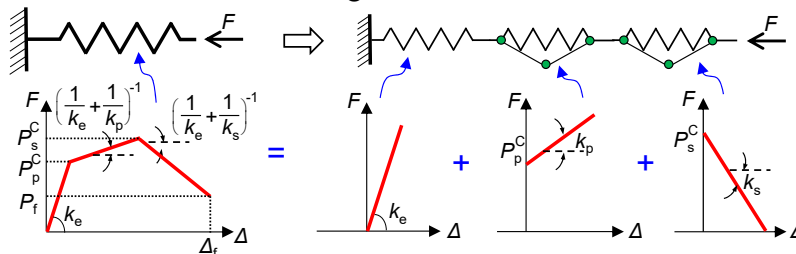


Fig. 1. Use of three springs to reproduce tri-linear behaviour of a spring. Note that k_s is negative.

2.2 Moment-rotation relationship of a multi-spring system

By applying the minimum total potential energy principle to a multi-spring system, the moment-rotation relationship of the system can be written as [2]:

$$M(\theta) = -\frac{\left(\sum_1^N K_I^j h_I\right)^2}{\sum_1^N K_I^j} \sin \theta \cos \theta + \sum_{I=1}^N K_I^j h_I^2 \sin \theta \cos \theta + \sum_{I=1}^N K_I^j h_I C_I^j \cos \theta - \frac{\left(\sum_1^N K_I^j h_I\right)\left(\sum_1^N K_I^j C_I^j\right)}{\sum_1^N K_I^j} \cos \theta \quad (4)$$

where K^j and C^j are matrixes of stiffnesses and preloading constants, respectively, containing the stiffness and preloading constant of each spring series I , the number of which is N ; and h_I is the height of spring series I measured from the centroid of the connected beam.

2.3 Instantaneous centre of rotation

The instantaneous centre of rotation (ICR) is defined as the point whose displacement is independent of section rotation. The loading condition of a spring series on a rotating section can be determined by its relative position to this point. Assuming the section is rotating in the positive clockwise direction, a spring series located above the ICR is under either increasing tension or compressive unloading. Conversely, it is under either increasing compression or tensile unloading if located below the ICR. The height and the displacement of the ICR can be derived as [2]:

$$h_{\text{ICR}} = \frac{\sum_1^N K_I^j h_I}{\sum_1^N K_I^j} \quad (5)$$

$$\Delta_{\text{ICR}} = -\frac{\sum_1^N K_I^j C_I^j}{\sum_1^N K_I^j} \quad (6)$$

In the initial stage, $C_I^j = 0$, and therefore, $\Delta_{\text{ICR}} = 0$, indicating the ICR is the zero displacement point. Subsequently, when one or more of the spring series yields, the stiffness and preloading constant of that spring series will change, and thus the height of the ICR will change.

2.4 Post-fracture behaviour

An energy-based method is proposed to determine the post-fracture behaviour of a steel joint. As shown in Fig. 2, after the fracture of a component in a multi-spring system, the new static equilibrium point is located on the M - θ curve of the post-fracture system, denoted by $M_{f,1}(\theta)$, where the spring series representing the fractured component is removed from the original multi-spring system. Moreover, as the propagation of fracture in a component is usually unstable and thus very rapid, the potential energy possessed by the post-fracture system just after returning to static equilibrium, $V_{f,1}$, is assumed to equal the total energy possessed by the pre-fracture system at incipient component fracture, $V_{f,0}$. This method can be repeated to model the successive fracture in the remaining components, thereby obtaining the entire post-fracture behaviour of the joint.

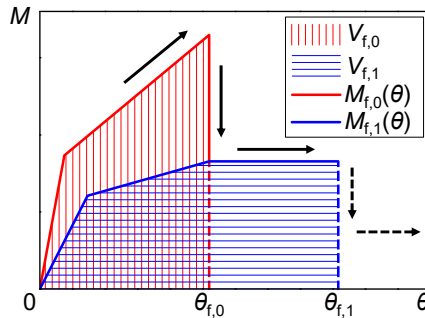


Fig. 2. Energy method to obtain the post-fracture moment-rotation curve.

3 VALIDATION OF THE GENERALISED COMPONENT METHOD

The proposed Generalised Component Model is potentially applicable to all types of steel joints and, in this section, is applied to three extended bolted end-plate connections tested at the University of Sydney, i.e., joints S10, S10BP and S20BP in [5], as shown in Fig. 3. The breakdown of these connections under pure bending into individual components is visualized in Fig. 4, with the corresponding components being (1) column web panel in shear, (2) column web in compression, (3) column web in tension, (4) column flange in bending (the backing plate is considered to be a part of the column flange), (5) end-plate in bending, and (10) bolts in tension.

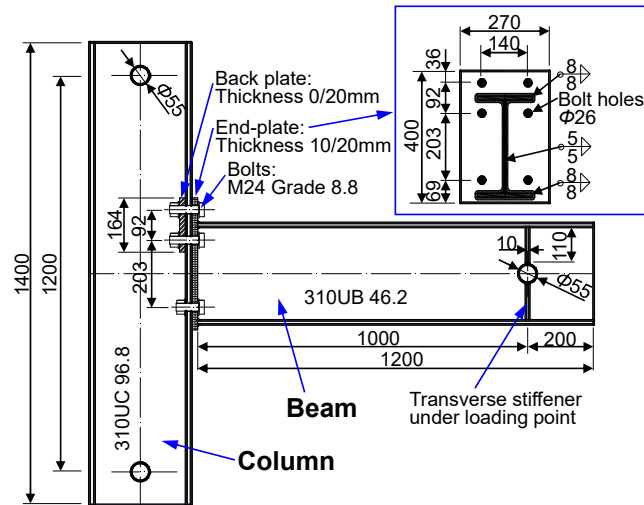


Fig. 3. Geometry of specimens (unit: mm).

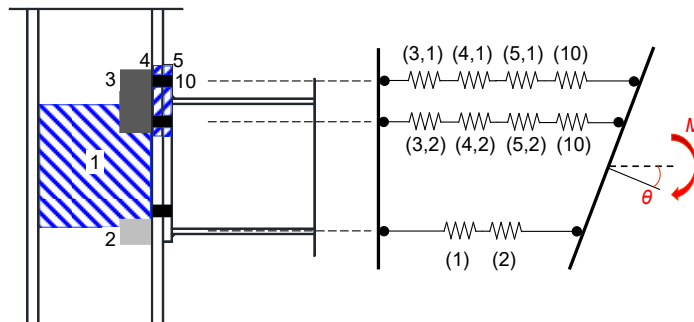


Fig. 4. Component identification and corresponding component model for bending.

For all components, the initial stiffness and the elastic limit are calculated according to Eurocode 3, and the component plastic stiffness is assumed to be a certain percentage of the component initial stiffness, which depends on the component type [6-7]. For components (1), (2), (3), (4) and (5), the plastic stiffness is reduced to 5%, 5%, 1%, 5% and 5% of the initial stiffness, respectively. For component (2), a post-ultimate softening stiffness of -1% of the component initial stiffness is also introduced, in order to take the post-ultimate ductile behaviour of the component into account. For component (10), a linear model is used to represent the brittle failure mode of the component. Figures 5 to 7 show the model predictions, which are in excellent agreement with the experimental results.

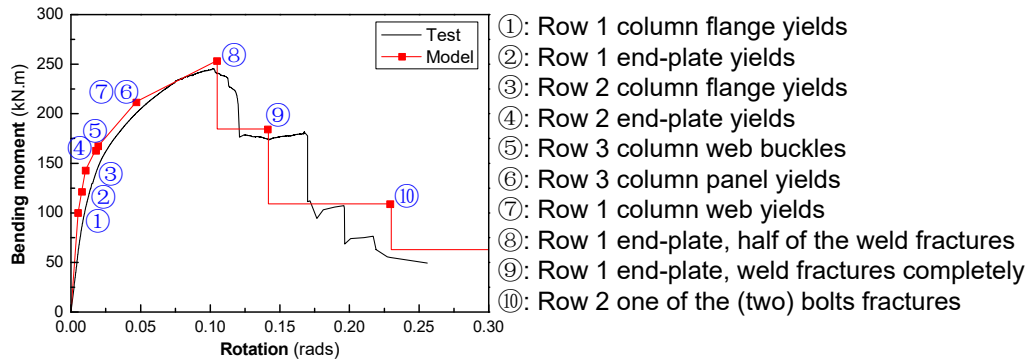


Fig. 5. $M-\theta$ curve of S10 obtained by the component model and comparison against test result.

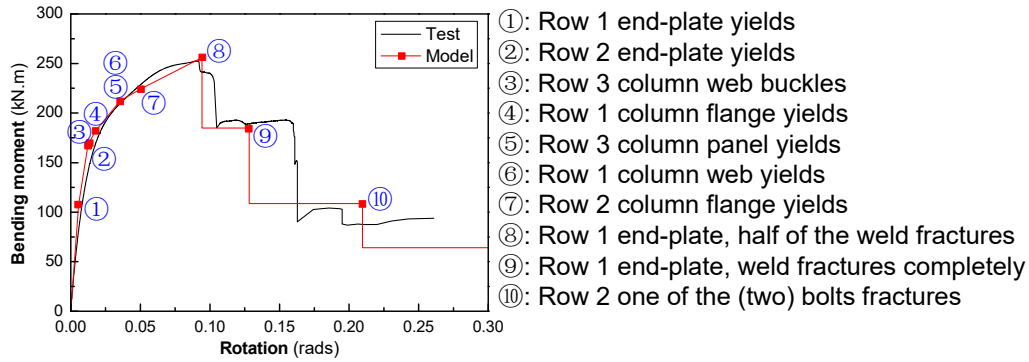


Fig. 6. $M-\theta$ curve of S10BP obtained by the component model and comparison against test result.

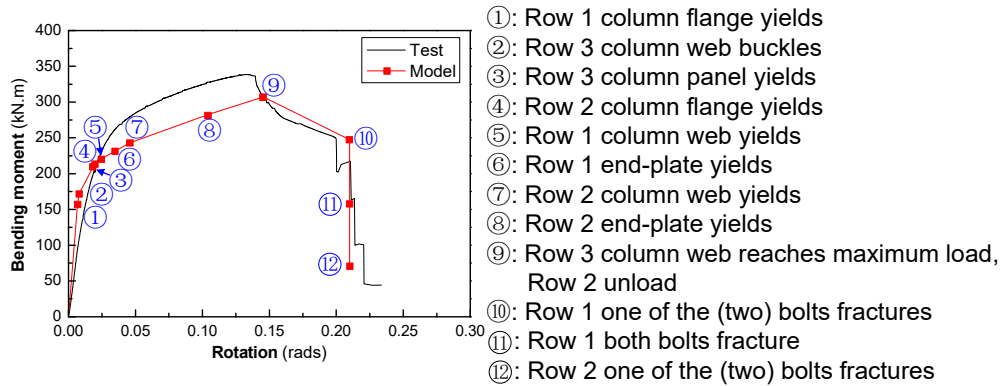


Fig. 7. $M-\theta$ curve of S20 obtained by the component model and comparison against test result.

4 COMPONENT MODEL FOR COLD-FORMED STEEL-STORAGE RACK BEAM-TO-UPRIGHT CONNECTIONS

Theoretical models have been developed based on the Component Method to predict the rotational stiffness of beam-to-upright connections in cold-formed steel storage racks, viz., boltless and bolted connections [8-10]. The typical configuration of the connections is presented in Fig. 8. This section summarises the identification, evaluation and assembly of basic deformable components contributing to the initial rotational stiffness of the connections.

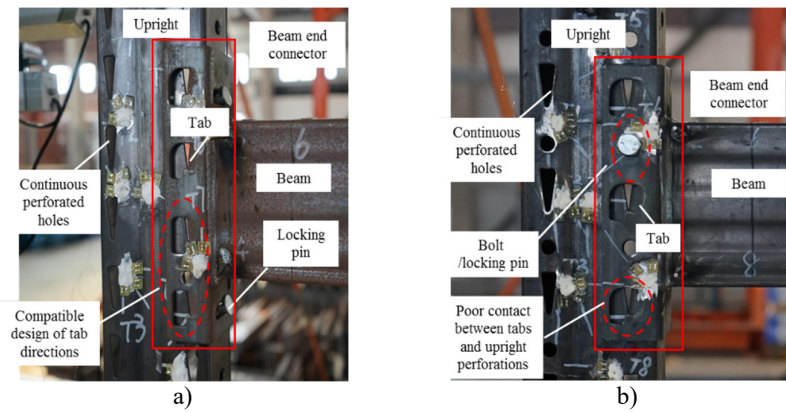


Fig. 8. Typical configuration of beam-to-upright connections in storage racks. a) Boltless connection; b) Bolted connection

4.1 Identification of key components and mechanical model description

In order to develop the mechanical model, the elementary deformable components contributing to the initial rotational stiffness are firstly identified. As observed from tests, it can be derived that:

- The *beam* end connector is assumed not to be in contact with the upright flange initially, whereas tabs and bolts are considered to be in contact with the upright wall at the early stage of loading.
- “Tab in bending” is an important component contributing to the connection rotation. However, for bolted connections, the component behaviours of tabs located above and below the rotation centre are not identical due to their different contact areas, as shown in Fig. 9 (a).
- With *the* installation of a bolt in the connection, the bearing deformation of plates in contact with the bolt is taken into account.
- The shear deformation of the bolt is negligible compared to the deformations of other components and is *ignored* in the model for predicting the initial stiffness of connections, as is the tensile deformation of the weld between the beam and the end connector.
- The *deformations*, caused by beam flange and web in compression, beam web in tension and upright web in compression, are not significant, and thus can be neglected.
- Except for plates in bending, bolted connections have similar deformable components as boltless connections, and thus the same equations can be used in evaluating the behaviour of these components.

Figure 9 illustrates the component model for bolted connections. The model for boltless connections is almost the same except that the deformable components relating to the bolt are not included. Based on the assumptions listed above, seven basic deformable components contributing to the initial stiffness of the connections are highlighted in Fig. 9, i.e. tab in bending (tb), upright wall in bearing (cwc), upright wall in bending (cwb), beam-end-connector in bending and shear (bcb), upright web in shear (cws) and plates in bearing (b-bcb, b-cwc). Except for column web in shear (cws) component, other components are dependent on the location of tabs and the bolt. Figure 9(b) shows the proposed component model, in which each component is characterised by an extensional linear-elastic equivalent spring. It should be noted that the location of the representative extensional springs, which means the calculation point of basic components, is the midpoint of the connecting length between tab and the upright perforation or between bolt and the upright perforation, as shown in Figs 9(a-b).

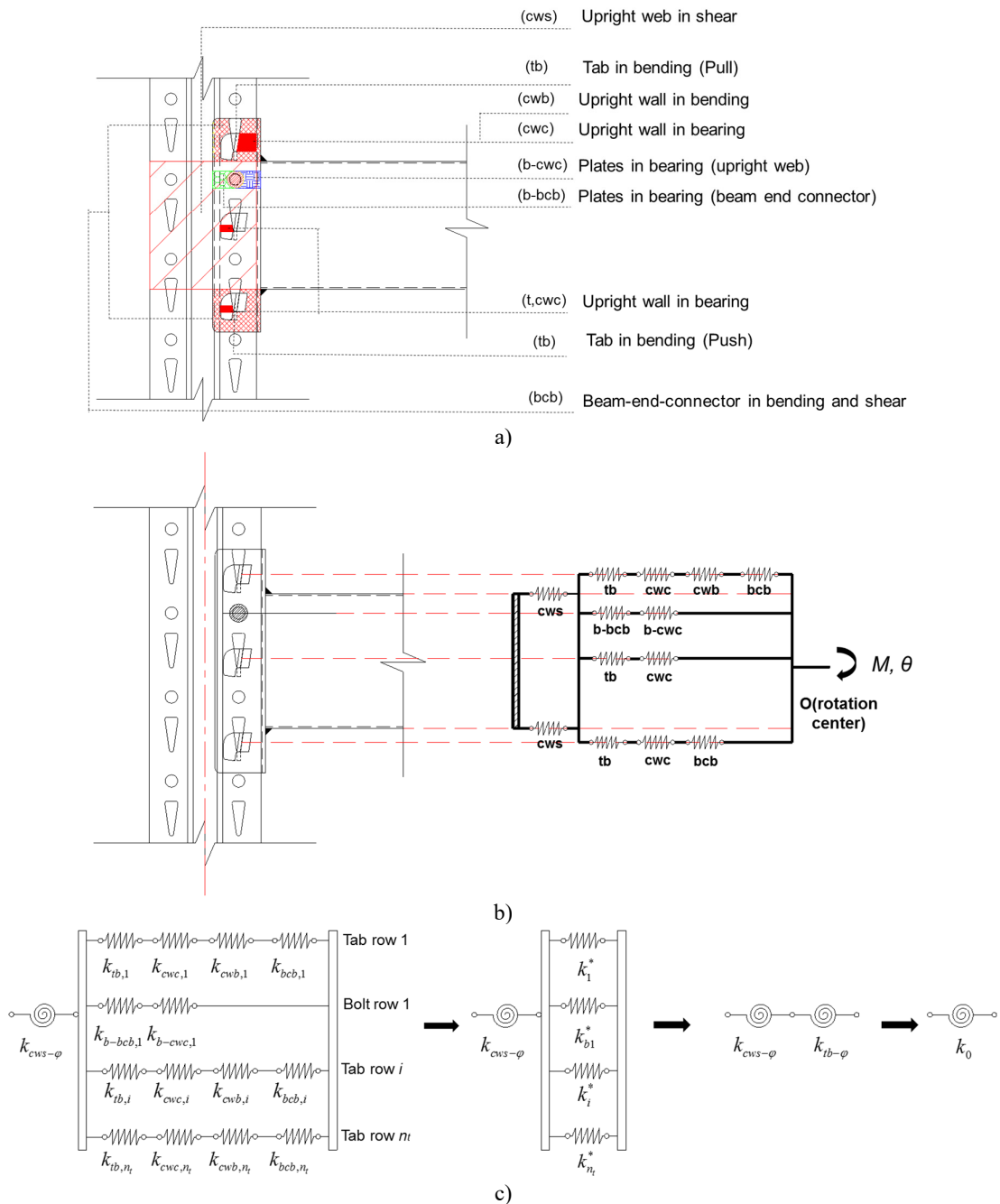


Fig. 9. Component model of beam-to-upright bolted connections. a) Component identification; b) Mechanical model; c) Assembly of key deformable components

4.2 Behaviour of individual components

The calculations of the extensional stiffness corresponding to the deformable components of the connections are summarised in Table 1. The “tab in bending” component is of great importance in predicting the behaviour of connections in cold-formed steel storage racks, and to derive the stiffness of the component an equivalent bending beam model was established [9]. Regarding bolted connections, components related to plates in bearing (b-bcb, b-cwc) have also been taken into account, and their stiffnesses are defined in Table 1 in accordance with the approach proposed in Eurocode 3 [1]. It is important to note that the tabs located below the rotation centre are in poor contact with the upright perforations during the loading process (see Fig. 9(a)). Therefore, the contact lengths between tabs and upright perforations, h_c and h_t (see Table 1, “Tab in bending”), are

determined by the assumed degree of connectivity between the tabs and the perforations under pull and push actions, respectively. For the joints considered in this study, if tabs are under pull action, the value of the contact length, h_c , is taken as 17mm, being the nominal length of the tab end. As has been explained above, the tabs of the bolted connections are in poor contact with upright perforations when under push action. Since nominally identical tabs and upright perforations are employed in all tested connections in this study, the length for pull action, h_t , is based on the average measured value of 4mm obtained from a selection of typical connections. Note that since the theoretical model is proposed to predict the initial rotational stiffness of the connections, it provides satisfactory accuracy to adopt the values of h_t measured at the initial stage of loading.

4.3 Evaluation of rotational stiffness

Based on the mechanical model presented in Fig. 9(b) and formulations for determining the extensional stiffness corresponding to each basic component illustrated in Table 1, the initial rotational stiffness of the steel storage rack beam-to-upright connection can be derived from a combination of the stiffnesses of individual basic components. Figure 9(c) shows the procedure for determining the initial rotational stiffness of the connection. Equation 7 presents the formula to calculate the stiffness of the equivalent extensional spring (“ i ” represents the number of tab row) relating to the tab rows. Equation 8 is the formula to determine the stiffness of the equivalent spring relating to the bolt row.

$$k_i^* = \frac{1}{\frac{1}{k_{tb,i}} + \frac{1}{k_{cwc,i}} + \frac{1}{k_{cwb,i}} + \frac{1}{k_{bcb,i}}} \quad (7)$$

$$k_{b1}^* = \frac{1}{\frac{1}{k_{b-bcb,i}} + \frac{1}{k_{b-cwc,i}}} \quad (8)$$

It should be noted that not all individual components may be relevant in calculating k_i^* from Eq. 7. In particular, k_{cwb} is assumed to be infinite in cases of upright walls below the rotation centre and k_{bcb} is only considered in cases where the part of beam-end-connector beyond the beam contains at least one tab.

The lever arm, L_i , of each equivalent linear spring k_i^* is derived on the basis that the resultant force of all equivalent springs is zero, as shown in Eq. 9, in which d_i is the deformation of equivalent spring k_i^* . The derivation of d_i is illustrated in Eq. 10, in which ϕ_0 is the rotation resulted from $k_{tb-\phi}$ (see Fig. 9(b)). Equation 11 assumes that tabs are equally spaced along the beam-end-connector, L_i represents the lever arm of the i th equivalent spring and d_{tab} refers to the spacing between two adjacent tabs.

$$\sum_{i=1}^n k_i^* d_i = 0 \quad (9)$$

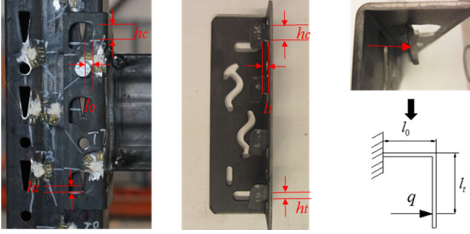
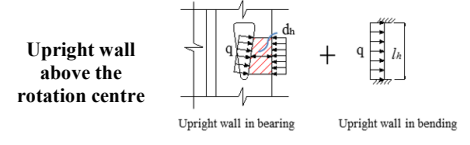
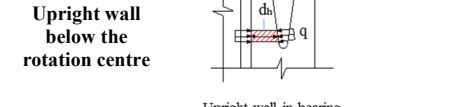
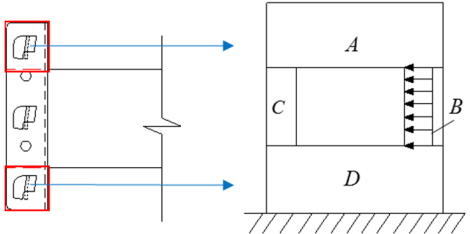
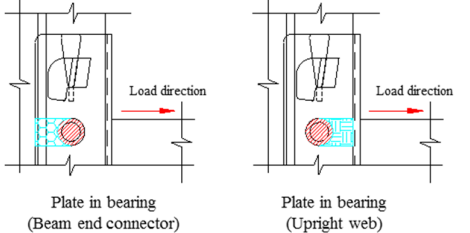
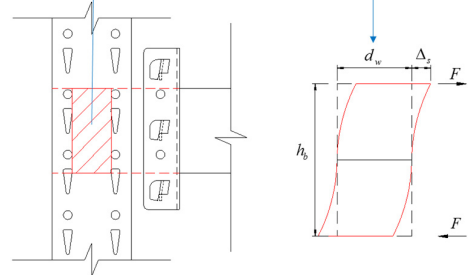
$$d_i = L_i \times \phi_0 \quad (10)$$

$$L_i - L_j = (j - i) \times d_{tab} \quad (11)$$

The equivalent overall *rotational* stiffness $k_{t-\phi}$ is derived from the following relationship:

$$k_{t-\phi} = \sum_{i=1}^n k_i^* L_i^2 \quad (12)$$

Table 1. Equations for stiffness of key deformable components [10].

Component	Stiffness of equivalent spring k	Schematic diagram
<p><i>Tab in bending</i></p>	$k_{tb} = \frac{Eh_c t_i^3}{4l_i^2 \times (l_i + 3l_0)} \text{ or } = \frac{Eh_t t_i^3}{4l_i^2 \times (l_i + 3l_0)}$ <p>l_i is the length of tab end in side view of the connection; l_0 is the length of tab end in front view of the connection; E is elastic modulus; t_i is thickness of tab; h_c and h_t are the contact lengths between tabs and upright perforations under pull and push actions respectively.</p>	 <p>Front view Side view Tab</p>
<p><i>Upright wall in bearing</i></p>	$k_{cwc} = \frac{Eh_t t_{up}}{d_h}$ <p>t_{up} is the thickness of the upright; d_h is the distance between the loading point of the resultant force and the edge of reaction areas.</p>	 <p>Upright wall above the rotation centre</p>
<p><i>Upright wall in bending</i></p>	$k_{cwb} = \frac{32Et_{up}d_h^3}{l_h^3}$ <p>l_h is the length of upright perforation.</p>	 <p>Upright wall below the rotation centre</p>
<p><i>Beam-end-connector in bending and shear</i></p>	$k_{becb} = \frac{1}{\frac{h_B^3}{384EI_B} + \frac{k}{2(k+1)} \left[\frac{h_B^2}{24EI_B} \left(\frac{3h_A}{2} + \frac{5h_B}{2} \right) + \frac{1.3h_B}{EA_B} \right] + \left[\frac{h_D^2}{12EI_D} \left(\frac{3h_A}{2} + 3h_B + 2h_D \right) + \frac{1.3h_D}{EA_D} \right] + \frac{h_B h_D}{8EI_D} (h_A + 2h_B + h_D)}$ $k = \left(\frac{w_B}{w_C} \right)^3 \frac{h_C^2 + 2.6w_C^2}{h_B^2 + 2.6w_B^2}; \quad I_j = w_j^3 t_{bec} / 12; \quad A_j = w_j t_{bec}$ <p>j refers to the Plate A, B, C and D; w_j is the width of Plate j; h_j is the height of Plate j; t_{bec} is the thickness of Plate j.</p>	 <p>Note: The cantilever wall is divided into four plates, named A, B, C and D, according to the edge of the opening.</p>
<p><i>Plates in bearing</i></p>	$k_{b-bcb} \text{ (or } k_{b-cwc}) = 12k_b k_r d f_u$ $k_b = 0.25e_b/d + 0.5 \leq 1.25$ $k_r = 1.5t_j/d_{M16} \leq 2.5$ <p>e_b is the distance from the bolt row to the free edge of the plate in the direction of load transfer; f_u is the ultimate tensile strength of the steel on which the bolt bears; t_j is the thickness of the bearing plate.</p>	 <p>Plate in bearing (Beam end connector) Plate in bearing (Upright web)</p>
<p><i>Upright web in shear</i></p>	$k_{cws} = \frac{Gt_{up}d_w}{h_b/2}$ $k_{cws-\varphi} = Gt_{up}d_w h_b$ <p>G is shear modulus; d_w is the width of web panel; h_b is the height of the beam.</p> <p>Note that $k_{cws-\varphi}$ is the rotational stiffness value of the rotational spring for upright web in shear, while k_{cws} is the axial stiffness value of the corresponding extensional spring.</p>	

Finally, combining the rotational stiffness of the column web in shear (cws) component ($k_{cws-\varphi}$) with the equivalent overall rotational stiffness relating to the tab rows ($k_{tb-\varphi}$), the initial rotational stiffness of the complete connection is determined as,

$$k_0 = \frac{1}{\frac{1}{k_{tb-\varphi}} + \frac{1}{k_{cws-\varphi}}} \quad (13)$$

The initial rotational stiffness (k_0) defines the slope of the elastic range of the moment-rotation relationship.

5 VALIDATION OF THE COMPONENT MODEL FOR RACK BEAM-TO-UPRIGHT CONNECTIONS

The above theoretical model for cold-formed steel-storage rack beam-to-upright connections is validated against experimental results presented in [10, 11]. The relationship between the theoretical initial rotational stiffness (k_0) and experimental initial rotational stiffness (k_E) is presented in Fig. 10. The line representing the mean value of the ratio is also provided. It can be seen from the figure that the results obtained from the proposed mechanical model are in excellent agreement with the experimental data for bolted connections, while for boltless connections the component model predicts slightly higher stiffnesses than observed in the experiments. Overall, the proposed mechanical model provides a good prediction of the initial rotational stiffness of boltless and bolted connections.

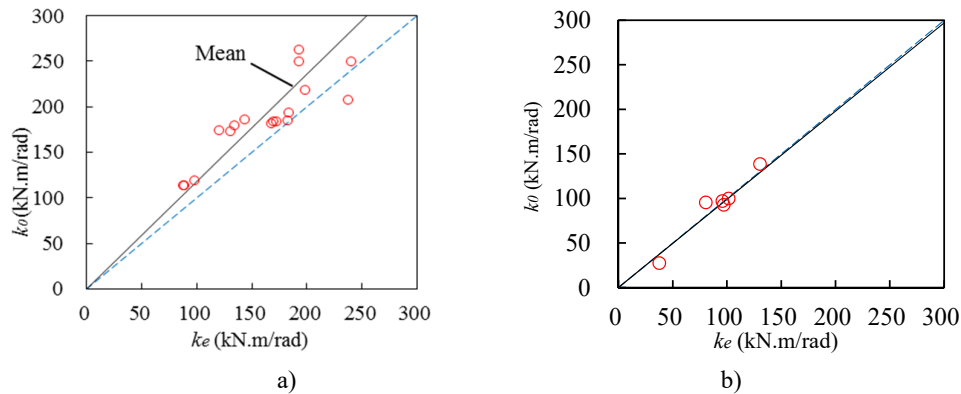


Fig. 10. Comparison between experimental and analytical values of initial rotational stiffness. a) Boltless connection; b) Bolted connection.

ACKNOWLEDGEMENT

The work presented in this paper was funded by the Australian Research Council under Discovery Project DP150104873.

REFERENCES

1. **CEN (European Committee for Standardization)**. EN 1993-1-8, Eurocode 3: design of steel structures, Part 1-8: design of joints. European Committee for Standardization, Brussels, 2010.
2. **Zhu, C., Rasmussen, K. J. R. and Yan, S.** Generalised Component Model for structural steel joints, *Journal of Constructional Steel Research*, 2019, 153, 330-342.
3. **Simões da Silva, L., Girão Coelho, A. M., and Lucena Neto, E.** Equivalent post-buckling models for the flexural behaviour of steel connections. *Computers & Structures*, 2000, 77, 615-624.
4. **Simões da Silva, L., and Girão Coelho, A. M.** A ductility model for steel connections. *Journal of Constructional Steel Research*, 2001, 57, 45-70.

5. **Zhu, C., Rasmussen, K. J. R., Yan, S., and Zhang, H.** Experimental full-range assessment of bolted moment end-plate connections, accepted for publication by American Society of Civil Engineers, Journal of Structural Engineering, 2019.
6. **Simões da Silva, L., Santiago, A., and Vila Real, P.** Post-limit stiffness and ductility of end-plate beam-to-column steel joints. Computers & Structures, 2002, 80, 515-531.
7. **Del Savio, A. A., Nethercot, D. A., Vellasco, P. C. G. S., Andrade, S. A. L. and Martha, L. F.** Generalised component-based model for beam-to-column connections including axial versus moment interaction." Journal of Constructional Steel Research, 2009, 65 (8), 1876-1895.
8. **Dai, L.** The Hysteretic Behaviour of Beam-to-upright Connections and Their Role in Predicting the Structural Response of Steel Storage Racks under Seismic Action. PhD thesis, The University of Sydney, Sydney, 2018.
9. **Zhao, X., Dai, L., Wang, T., Sivakumaran, K. S., Chen, Y.** A theoretical model for the rotational stiffness of storage rack beam-to-upright connections. Journal of Constructional Steel Research, 2017, 133, 269-281.
10. **Dai, L., Zhao, X., Rasmussen, K. J. R.** Flexural behaviour of steel storage rack beam-to-upright bolted connections. Thin-Walled Structures, 2018, 124, 202-217.
11. **Zhao, X, Wang, T, Chen, Y, Sivakumaran, K. S.** Flexural behavior of steel storage rack beam-to-upright connections. Journal of Constructional Steel Research 2014, 99:161-75.